BIOCHEMISTRY
including biophysical chemistry & molecular biology

ARTICLE

pubs.acs.org/biochemistry

Amyloid of the *Candida albicans* Ure2p Prion Domain Is Infectious and Has an In-Register Parallel β-Sheet Structure

Abbi Engel,[†,§] Frank Shewmaker,[†] Herman K. Edskes,[†] Fred Dyda,[‡] and Reed B. Wickner*[,†]

[†]Laboratory of Biochemistry and Genetics and [‡]Laboratory of Molecular Biology, National Institute of Diabetes and Digestive and Kidney Diseases, National Institutes of Health, Bethesda, Maryland 20892-0830, United States

[§]Department of Biochemistry and Molecular Biology, Georgetown University School of Medicine, Washington, D.C. 20057, United States

Supporting Information

ABSTRACT: Ure2p of *Candida albicans* (Ure2^{albicans} or *Ca*Ure2p) can be a prion in *Saccharomyces cerevisiae*, but Ure2p of *Candida glabrata* (Ure2^{glabrata}) cannot, even though the Ure2^{glabrata} N-terminal domain is more similar to that of the *S. cerevisiae* Ure2p (Ure2^{cerevisiae}) than Ure2^{albicans} is. We show that the N-terminal N/Q-rich prion domain of Ure2^{albicans} forms amyloid that is infectious, transmitting [URE3alb] to *S. cerevisiae* cells expressing only *C. albicans* Ure2p. Using solid-state nuclear magnetic resonance of selectively labeled *C. albicans* Ure2p$^{1-90}$, we show that this infectious amyloid has an in-register parallel β-sheet structure, like that of the *S. cerevisiae* Ure2p prion domain and other *S. cerevisiae* prion amyloids. In contrast, the N/Q-rich N-terminal domain of Ure2^{glabrata} does not readily form amyloid, and that formed upon prolonged incubation is not infectious.

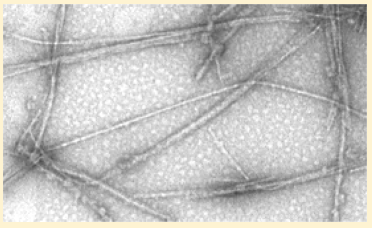

A prion is an infectious protein, a protein that can transmit an infection without a required nucleic acid. The nonchromosomal genes [URE3] and [PSI+] were identified as prions of Ure2p and Sup35p of *Saccharomyces cerevisiae* on the basis of their unique genetic properties: (i) reversible curability, (ii) prion generation induced by overproduction of the corresponding protein, and (iii) phenotype of prion similar to that of mutants in the corresponding gene needed for maintaining the prion.[1] [PIN+] was detected as a nonchromosomal factor needed for inducing the appearance of [PSI+] via overproduction of Sup35p[2] and shown to be a prion of Rnq1p by the genetic criteria given above.[3] The [SWI+] and [OCT+] prions[4,5] were uncovered because their respective proteins, Swi1p and Cyc8p, were found, when overproduced, to have properties like those of the [PIN+] prion. [MOT3+] was found in a screen of proteins with Q/N-rich regions.[6] Each of these prions is based on self-propagating amyloid formation by a Q/N-rich protein domain (the prion domain) (e.g., refs 7−9).

Prions of Ure2p from other *Saccharomyces* species have also been described,[10−13] but Ure2p of *Saccharomyces castellii* cannot be a prion in *S. cerevisiae*.[13] When expressed in *S. cerevisiae*, the Ure2p's of *Candida albicans*, *Kluyveromyces lactis*, and *Schizosaccharomyces pombe* were reported to be unable to form a prion, even after overexpression of the respective putative prion domain,[11] and the *K. lactis* Ure2p cannot be a prion in *K. lactis*.[14] Sup35 domains N, M, and C, from N- to C-terminus, are the prion domain (necessary for normal mRNA turnover[15]), a charged middle domain, and the C domain necessary for translation termination, respectively.[9] The N-terminal domains of Sup35 of several yeast species, including *C. albicans*, can be prion domains when fused to the *S. cerevisiae* C domain.[16−18] This is a significant qualification because the prion forming ability of prion domains of Ure2p, Sup35p, and HET-s is consistently inhibited by the presence of the remainder of the molecule,[8,19,20] perhaps by some stabilizing effect. Hsp104 is a disaggregating chaperone that is necessary for the propagation of each of the amyloid-based yeast prions.[2,4,5,21,22] Its role appears to be that of breaking amyloid filaments to form new prion "seeds".[23] The *C. albicans* Hsp104 homologue is capable of substituting for the *S. cerevisiae* Hsp104 in propagating [PSI+], suggesting that *C. albicans* may have an environment compatible with prion propagation.[24]

Amyloid is a filamentous protein polymer that is rich in β-sheet, shows special dye binding properties, and is usually more protease resistant than the non-amyloid form of the protein. The amyloids of the prion domains of *S. cerevisiae* Ure2p, Sup35p, and Rnq1p are infectious,[25−28] and each has an in-register parallel β-sheet structure.[29−31] Measurements of mass per unit length for each are consistent with this structure and inconsistent with a β-helix model,[32−34] and the fact that the Ure2p and Sup35p prion domains may each be shuffled in sequence and yet still form prions predicts the same structure.[35−37] The in-register parallel β-sheet structure also provides a simple explanation of prion variants, with the different locations of the folds of the β-sheet "inherited" by new molecules joining the end of the filament.[38,39] In brief, the same hydrogen bonds and hydrophobic interactions between identical side chains of residues aligned in the parallel in-register β-sheets that hold the β-

Received: January 27, 2011
Revised: March 26, 2011
Published: June 02, 2011

Table 1. *C. albicans* and *C. glabrata* URE2 Expression Plasmids with Primers Used for Their Construction[a]

plasmid	*URE2* expression construct	5′ primer	3′ primer
pAE1	*URE2*^{glabrata}-H6 (full-length)	HE297, TAAGGATCCCAAATGGGTGACT-CACGCAAT	AE68, GTTCTCGAGTTA*ATGGTGATGGTGATGATG*-CTCTCCGCGAAGGGC
pAE2	*URE2*$^{glabrata\ 1-100}$-H6 (PD)	HE297, TAAGGATCCCAAATGGGTGACTC-ACGCAAT	AE88, CTTCTCGAGTTA*ATGGTGATGGTGATGAT*-GATACTCCATCGGGTTGAATT
pAE3	*URE2*$^{albicans\ 1-89}$-H6 (PD)	AE100, AACTCTAGAAATAATTTTGTTTAACTTT-AAGAAGGAGATCTATGATGTCTACTGATCAAC	AE101, CTTCTCGAGTTA*ATGGTGATGGTGATGAT*-GTTGTTGTTGTTGAGTAGAAGC
pAE4	*URE2*^{albicans}-H6 (full-length)	AE100, AACTCTAGAAATAATTTTGTTTAACTTTAA-GAAGGAGATCTATGATGTCTACTGATCAAC	AE102, CTTCTCGAGTTA*ATGGTGATGGTGATGAT*-GATCTCCACGTAAAGCGCGTTT
pAE5	*URE2*$^{albicans\ 1-90}$-H6 (PD)	NdeAlb*URE2*, AAAACATATGATGTCTACTG-ATCAACATAT	cXhoAlb*URE2*, TGGCTCGAGTTTA*ATGGTGATGATGGT*-*GATG*TCTTGATTGTTGTTGTTGAGTAGAAGCTT

[a] All expression plasmids are derivatives of pUB6 [gift from Ulrich Baxa; modified pET17-b (Novagen)] except for pAE5, which is derived from pET21-b (Novagen). Italics indicate the six-His tag; underlined portions are restriction sites.

strands in-register will direct the monomer joining the end of the filament to acquire the same conformation as the other molecules already in the filament. The location of turns (folds of the sheet) and the extent of β-sheet structure will be faithfully propagated but may differ among prion variants.

We have found that the full-length *C. albicans* Ure2 protein can form a [URE3] prion in *S. cerevisiae*, but the *Candida glabrata* Ure2p cannot.[40] Here we show that the *C. albicans* Ure2p prion domain forms amyloid more readily than that of *C. glabrata*, which forms amyloid only over years. Moreover, the *C. albicans* Ure2p prion domain amyloid is infectious, transmitting [URE3alb] to *S. cerevisiae* cells expressing *C. albicans* Ure2p. We present solid-state NMR data suggesting that, like the *S. cerevisiae* prion domains, the *C. albicans* Ure2p prion domain forms amyloid with an in-register parallel β-sheet structure.

EXPERIMENTAL PROCEDURES

Yeast Strains and Media. *S. cerevisiae* strains BY302 (*MAT***a** *his3 leu2 trp1 CaURE2* P_{DAL5}*:ADE2* P_{DAL5}*:CAN1 kar1*) and BY304 (*MAT***a** *his3 leu2 trp1 CgURE2* P_{DAL5}*:ADE2* P_{DAL5}*:CAN1 kar1*) contain the *cerevisiae URE2* ORF perfectly replaced by the *C. albicans* and *C. glabrata URE2* ORFs, respectively.[40] Strain YHE1161 is BY302 carrying [URE3alb].[40] Rich medium (YPAD) contains 1% yeast extract, 2% peptone, 2% dextrose, 2% agar, and 0.4 g/L adenine sulfate. Minimal medium (SD) contains 0.67% Difco Yeast Nitrogen Base without amino acids, 2% dextrose, and 2% agar. YES medium, for scoring [URE3], contained 0.5% yeast extract, 3% dextrose, 30 mg/L tryptophan, and 2% agar.

Plasmid Constructions. *C. albicans* and *C. glabrata URE2* expression vectors were all constructed in pET vector backbones with either the N-terminal domain (or "PD") or the full-length proteins attached to a C-terminal six-His tag (Table 1).

Transfection. Strains BY302 and BY304 were used as transfection recipients using the method of Brachmann et al.[27,41] Clones were selected for transformation using pRS425.[42] Filaments or extracts of [URE3alb.] strain YHE1161[40] were sonicated three times for 20 s each at output level 2−3 with a 20−30% duty cycle (Branson Sonifier 250) with cooling on ice between sonications.

Purification of *C. albicans* and *C. glabrata* Ure2p and Ure2p N-Terminal Domains. Plasmids in BL21(DE3) RIPL (Stratagene) were grown overnight with 34 μg/mL chloramphenicol, 50 μg/mL streptomycin, and 100 μg/mL ampicillin and inoculated into LB medium or synthetic complete medium[43] with 200 mg/L Ile-1-^{13}C or Val-1-^{13}C or 1 g/L Ala-3-^{13}C for site-specific labeling. Mass spectrometry showed that Ala residues were 60% labeled, and no significant leakage of label into other amino acids was detected. The latter medium without amino acids, but containing 2 g/L $^{15}NH_4Cl$ and 5 g/L uniformly ^{13}C-labeled glucose, was used for uniform labeling of *Ca*Ure2p$^{1-90}$. At an A_{600} of ~0.6−1.0, 1 mM isopropyl β-D-thiogalactosidase (IPTG) was added, and after growing for an additional 4 h, cells were harvested. *Ca*Ure2p$^{1-90}$ or *Cg*Ure2p$^{1-100}$ was obtained from bacteria lysed by vigorous agitation with 6 M guanidine-HCl, 0.1 M Tris, and 150 mM NaCl (pH 8.0−8.5) and incubation at room temperature for 1−2 h. Full-length protein of both *C. glabrata* and *C. albicans* was obtained by lysing cells using a French pressure cell in 50 mM $NaHPO_4$ and 300 mM NaCl (pH 8) with Roche protease inhibitors (complete EDTA-free) . Lysates were cleared of cell debris by ultracentrifugation at 30000 rpm for 30−60 min (Beckman-Coulter Optima L-90k Ultracentrifuge, type 45Ti rotor). Cleared lysates were incubated with nickle-nitrilotriacetic acid (NiNTA) agarose (Qiagen) at room temperature with gentle agitation, loaded into a glass column (Biorad), and washed with urea buffer (8 M urea, 0.1 M Tris, and 150 mM NaCl) for the N-terminal fragments or 50 mM $NaHPO_4$ and 300 mM NaCl (pH 8) for the full-length proteins. After the column had been washed with the same buffer with 20 mM imidazole, proteins were eluted with the same buffer with 200 mM imidizole. Protein concentrations were roughly determined with a 4 to 12% NuPAGE Bis-tris gel (Invitrogen) stained with SimplyBlue Safestain (Coomassie G-250 stain, Invitrogen) and by BCA assay (Pierce).

If necessary, further purification used a Q-sepharose column (HighQ, Bio-Rad). Fractions containing protein were diluted 5-fold with zero-salt urea buffer (8 M urea and 50 mM Tris) and loaded onto the Q-column. The column was washed with the same zero-salt urea buffer. Protein was eluted with a gradient from 0 to 200 mM NaCl added in the same buffer.

Amyloid Formation. Selected fractions were pooled, concentrated, and dialyzed against 50 mM Tris-HCl and 150 mM NaCl (pH 8) to induce amyloid formation. Filaments were formed at room temperature with agitation for 2 days to 1 week. A variety of buffers were tested in an effort to induce filament formation by *C. glabrata* Ure2p$^{1-100}$. The following buffers were tested: 5 mM KPO_4 and 150 mM NaCl (pH 6.8); 50 mM Tris-HCl and 300 mM NaCl (pH 8); 3 M urea, 0.1 M Tris-HCl, and 150 mM NaCl (pH 8.3); 20 mM Tris-HCl and 200 mM KCl (pH 8); and

50 mM Tris-HCl and 150 mM NaCl (pH 8). Prolonged incubation of *C. glabrata* Ure2p$^{1-100}$ produced only limited amyloid (see Results), and SDS gel analysis of the still soluble material showed no change in the protein pattern after 2 years.

X-ray Fiber Diffraction. Sample preparation, X-ray fiber diffraction, and data analysis were conducted as described previously.[31]

Electron Microscopy. Ten microliters of a suitable dilution of filaments was deposited on a carbon-coated copper grid, washed once with water, and stained with 2% uranyl acetate for 2 min. The stain was blotted off and the grid allowed to air-dry, and images were obtained using an FEI Morgagni transmission electron microscope at 80 kV.

Solid-State NMR. Solid-state NMR experiments on selectively labeled *Ca*Ure2p$^{1-90}$ were conducted on a Varian InfinityPlus spectrometer at 9.39 T (100.4 MHz ^{13}C NMR frequency) using magic angle spinning (MAS) in 3.2 mm rotors at room temperature. Although some cooling was used, rotors spun at 20 kHz may warm to ~40 °C. One-dimensional spectra were recorded at 20 kHz MAS using ^{1}H−^{13}C cross polarization[44] and two-pulse phase-modulated ^{1}H decoupling.[45] The dipolar recoupling measurements were taken at 20 kHz MAS using the PITHIRDS-CT method[46] with pulsed spin-lock detection for improved signal-to-noise ratios.[47] *Ca*Ure2p$^{1-90}$ filament samples were washed with water, lyophilized, and packed in thick-walled 3.2 mm rotors. ^{13}C T_2 values under PITHIRDS-CT measurement conditions were measured by incrementing the total pulse sequence length while keeping the effective recoupling time equal to zero, to ensure that no less than 25% of the signal remained at the end of the dipolar recoupling period.

PITHIRDS-CT data for an unlabeled sample of *Ca*Ure2p$^{1-90}$ were measured (Figure 3A) and used to correct for the 1% natural abundance ^{13}C, assuming linear signal decay: natural abundance signal = $S_{na} = 100 - 0.2t$, where t is the effective dipolar dephasing time in milliseconds. The number of natural abundance ^{13}C nuclei per *Ca*Ure2p$^{1-90}$ molecule, N_{na}, is 0.011 (total sites minus labeled nuclei), where total sites is 139 carbonyls or 30 methyls. The number of labeled nuclei, N_{label}, was 2 for Ile-1-^{13}C, 5 for Val-1-^{13}C, and 2 for Ala-3-^{13}C. The fraction of natural abundance ^{13}C (F_{na}) equals $N_{na}/(N_{label} + N_{na})$. Experimentally determined ^{13}C T_2 values were used to correct the magnitude of the natural abundance signal when its T_2 differed from that of the specifically labeled sample. Raw PITHIRDS-CT data were corrected according to the following: $S(t) = [S_{raw} - F_{na}(100 - 0.2t)]/(1 - F_{na})$.

Two dimensional (2D) NMR experiments with uniformly ^{15}N- and ^{13}C-labeled rehydrated amyloid filaments of *Ca*Ure2p$^{1-90}$ in 3.2 mm rotors were conducted at 17 kHz MAS. The mixing period comprised 48 rotor periods (2.82 ms) of finite pulse RFDR (radiofrequency-driven recoupling) with 18 μs ^{13}C π-pulses. Continuous proton decoupling at 110 kHz was used during the mixing period, and TPPM (two pulse phase-modulated) decoupling,[45] also at 110 kHz, during the t1 and t2 periods. 2D NMR data were analyzed using NMRPipe[48] and are displayed relative to tetramethylsilane using an Ala-1-^{13}C standard.

RESULTS

***C. albicans* Ure2p$^{1-90}$ Readily Forms Amyloid.** The N-terminal domain of the *C. albicans* Ure2p is presumed to be the prion domain based on its Q/N richness and the finding that its overproduction induces the de novo appearance of [URE3].[40] We chose to study *Ca*Ure2p$^{1-90}$ because beyond residue 90, homology with the C-terminal domain of the *S. cerevisiae* Ure2p begins. *Ca*Ure2p$^{1-90}$-H_6 was purified under denaturing conditions from *E. coli* (see Experimental Procedures) and allowed to form filaments in the absence of denaturant. Filaments formed within a few days of gentle agitation at room temperature in 50 mM Tris-HCl (pH 8.0) and 150 mM NaCl (Figure 1). Fibrils of *Ca*Ure2p$^{1-90}$-H_6 were straight, apparently unbranched, and ~6 nm in diameter, with frequent lateral association (Figure 1). Some "twisted pairs" were occasionally observed (Figure 1A). These filaments exhibited yellow-green birefringence upon being stained with Congo red (Figure 1B), another trait typical of amyloid.

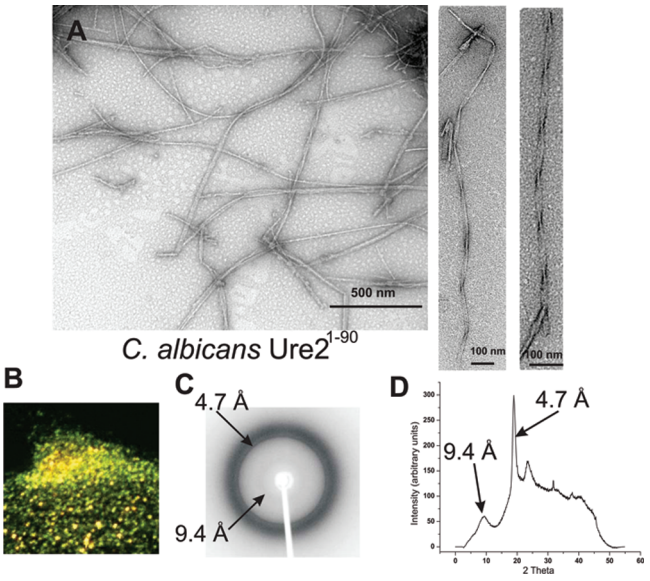

Figure 1. Ure2p$^{1-90}$ of *C. albicans* forms amyloid in vitro. (A) Electron micrographs of negatively stained filaments of *C. albicans* Ure2p$^{1-90}$. Filaments average ~6 nm in diameter. Examples of filaments showing a twisted appearance are shown on the right. (B) Yellow-green birefringence of Congo red-stained filaments of *Ca*Ure2p$^{1-90}$ viewed with a cross-polarizing microscope. (C) X-ray fiber diffraction of filaments of *Ca*Ure2p$^{1-90}$. Diffraction rings due to spacings of 4.7 and 9.4 Å are indicated. (D) Plot of the circular average of diffraction intensity.

X-ray fiber diffraction of the *C. albicans* Ure2p$^{1-90}$ fibers shows an intense sharp band at 4.7 Å and a broader band centered at 9.4 Å (Figure 1C,D). This pattern is diagnostic of β-sheet structure with the 4.7 Å peak due to reflections between adjacent β-strands and the 9.4 Å peak reflecting either the distance between neighboring β-sheets or possibly the distance between alternate β-strands (2 Å × 4.7 Å).

In contrast to the rapid formation of amyloid filaments by the *C. albicans* Ure2 N-terminal domain, that of *C. glabrata* only slowly and partially did so, in spite of many attempts under a variety of buffer conditions. After incubation for ~2 years at 4 °C, filaments of *C. glabrata* Ure2p$^{1-100}$ were observed, but the bulk of the protein remained soluble. Even seeding with a sonicated portion of these filaments did not promote filament formation after incubation for an additional 2 months in Tris or potassium phosphate buffers. X-ray fiber diffraction of the fibers formed showed a typical β-sheet pattern, and the fibers showed birefringence upon being stained with Congo red (not shown). Full-length *C. glabrata* Ure2p did not form detectable amyloid under the conditions used.

Table 2. *C. albicans* Prion Domain (Ure2p$^{1-90}$) Filaments Are Infectious[a]

recipient strain	infection material	number tested	number Ade+	number curable	average percent infection
BY302, *S. cerevisiae URE2*^{albicans}	none	303	17	0	0[b]
	*Ca*Ure2p$^{1-90}$ filaments	295	59	21	7[b]
	soluble *Ca*Ure2p$^{1-90}$	144	0	0	0
	BSA	144	3	0	0
	*Sc*Ure2$^{1-89}$ filaments	144	3	0	0
	full-length *Ca*Ure2p	144	3	0	0
	YHE1161 lysate ([URE3alb])	310	56	41	13[b]
BY304, *S. cerevisiae URE2*^{glabrata}	none	144	53	0	0
	*Cg*Ure2p$^{1-100}$ filaments	144	38	0	0
	soluble *Cg*Ure2p$^{1-100}$	144	63	0	0
	BSA	144	24	0	0
	*Sc*Ure2p$^{1-89}$ filaments	144	33	0	0
	full-length *Cg*Ure2p	144	41	0	0

[a] Spheroplasts of the indicated strain were transformed with pRS425 (*LEU2* 2 μm DNA) in the presence of freshly sonicated amyloid filaments of full-length Ure2p^{albicans} (5 μg), Ure2p^{glabrata} (3 μg), or Ure2p$^{cerevisiae\ 1-89}$ (30 μg) or filaments of Ure2p$^{albicans\ 1-90}$ (20 μg), Ure2p$^{glabrata\ 1-100}$ (3 μg), or soluble Ure2p$^{albicans\ 1-90}$ (20 μg) or Ure2p$^{glabrata\ 1-100}$ (6 μg). An extract of [URE3alb] strain YHE1161 (100 μg) was also used. Leu+ clones were tested for Ade+. Ade+ clones were tested for curability on 3 mM guanidine. [b] Average taken from three separate infection experiments.

C. albicans Ure2p$^{1-90}$ Filaments Are Infectious, Producing Several [URE3^{Ca}] Variants. Ure2p is a negative regulator of nitrogen catabolism, inhibiting the transcription of genes for transporters and enzymes needed for the utilization of poor nitrogen sources when a good nitrogen source is available (reviewed in refs 49 and 50). Transcription of *DAL5*, encoding the alantoate transporter, is particularly strongly repressed by Ure2p action.[51] By replacing the *ADE2* promoter with that of *DAL5*, we can use adenine auxotrophy (and red colony color on adenine-limiting media) as a sign of Ure2p activity.[27,52] Thus, [URE3] clones are Ade+ and white because of Ure2p inactivity, while [ure-o] clones are Ade− and red.

Various sonicated filament preparations were introduced[27] into *S. cerevisiae* strains in which the *URE2* gene had been replaced by that of *C. albicans* (BY302) or *C. glabrata* (BY304).[40] Cells that have taken up a DNA plasmid (pRS425) are selected as Leu+ colonies, and these are tested on Ade− plates. Those that are Ade+ (possible [URE3] transfectants) are grown on 3 mM guanidine to test for curing to confirm that the Ade+ is due to prion infection (Table 2). Guanidine inhibits Hsp104,[53] a disaggregating chaperone required for propagation of [URE3alb][40] as it is for other yeast prions. We found that a substantial portion of Leu+ clones had acquired [URE3alb] after infection with either filaments of *Ca*Ure2p$^{1-90}$ or an extract of [URE3alb] strain YHE1161 (Table 2). Infection required that the cell's *URE2* gene encode the same Ure2p as the infecting material, so *S. cerevisiae* Ure2p$^{1-89}$ (*Sc*Ure2p$^{1-89}$) filaments and *C. glabrata* Ure2p$^{1-100}$ (*Cg*Ure2p$^{1-100}$) filaments were not infectious for cells carrying *C. albicans URE2* (Table 2).

This infectivity of *Ca*Ure2p$^{1-90}$ filaments shows that Ure2p$^{1-90}$ includes the prion domain and is consistent with the ability of overexpression of this region to induce [URE3alb] formation in vivo.[40] Restreaking Ade+ [URE3alb] clones on adenine-limiting medium showed that the transfectants harbored an array of prion variants, differing in their stability and in the intensity of the Ade+ phenotype (Figure 2), similar to results observed for *S. cerevisiae* Ure2p filaments.[27]

Solid-State NMR Studies of *C. albicans* Ure2p$^{1-90}$ Amyloid. The infectivity of the *Ca*Ure2p$^{1-90}$ filaments implies that the structural studies we report here are relevant to the prion

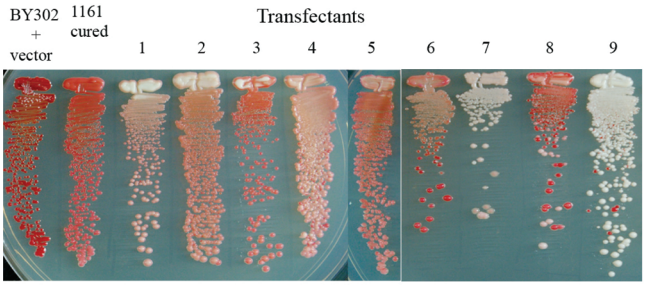

Figure 2. Ade+ [URE3alb] transfectants of BY302 were restreaked on YES (adenine-limiting medium). A red colony color indicates adenine deficiency. The differences in stability and color intensity indicate prion variant differences.

phenomenon. One-dimensional NMR spectra of dry fibrils of *Ca*Ure2p$^{1-90}$ labeled with Val-1-^{13}C, Ile-1-^{13}C, or Ala-3-^{13}C or unlabeled (natural abundance) are shown in Figure 3. Note that we have shown that the infectivity of amyloid fibrils of Ure2p^{cerevisiae} and Sup35NM is unaffected by drying.[54] The Ile-1-^{13}C-labeled amyloid showed a major peak (85%) at 172.6 ppm, whereas the chemical shift expected for random coil structure is 174.7 ppm.[55] For Val-1-^{13}C-labeled *Ca*Ure2p$^{1-90}$ amyloid, the major peak (68%) was at 171.9 ppm while the random coil value is 174.6 ppm. In general, carbonyl carbon resonance frequencies are shifted to lower values for residues in β-sheet structure and shifted up for α-helical residues.[55] These results indicate that most Ile and Val residues are in β-sheet structure. The X-ray fiber diffraction studies (above) indicate that β-sheet structure is more extensive than the few residues that could be examined individually by solid-state NMR.

In an amyloid with parallel in-register β-sheet structure, each residue is aligned in a row of identical residues extending along the long axis of the fibril. Therefore, if a particular amino acid, isoleucine, for instance, is fully labeled specifically in the carbonyl carbon (Ile-1-^{13}C), then the distance from each ^{13}C label to the nearest neighbor ^{13}C will be the 4.7 Å distance between main chains in the β-sheet[56,57] (reviewed in ref 58). In other forms of β-sheet (antiparallel, β-helix, or parallel out of register), the

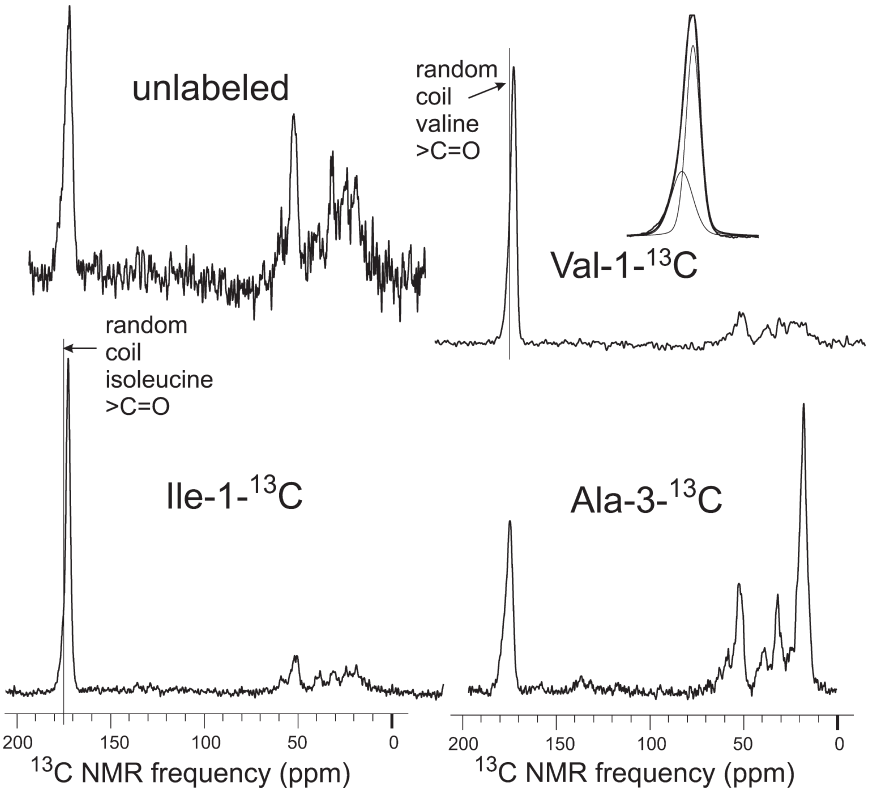

Figure 3. One-dimensional solid-state NMR spectra of *C. albicans* Ure2p$^{1-90}$ either unlabeled or labeled with Val-1-^{13}C, Ile-1-^{13}C, or Ala-3-^{13}C. The inset at the top right shows a deconvolution of the Val-1-^{13}C peak.

distance is far greater than 4.7 Å. This distance is measured by a dipolar recoupling experiment, such as the PITHIRDS-CT method used here.[46] In this experiment, the rate of signal decay is roughly proportional to the inverse of the cube of the distance from one labeled atom to its nearest labeled neighbor.

An amyloid sample of *Ca*Ure2p$^{1-90}$ labeled with Ile-1-^{13}C exhibited signal decay reflecting a nearest neighbor distance of ~5 Å indicating a parallel in-register structure (Figure 4A). Approximately 1.1% of all carbon is ^{13}C, so that the same experiment can be conducted using unlabeled amyloid. Of course, in this case, the nearest neighbor ^{13}C will nearly always be quite distant, and accordingly, a very slow signal decay was observed (Figure 4A). Val-1-^{13}C-labeled *Ca*Ure2p$^{1-90}$ amyloid exhibited an apparent biphasic signal decay curve, suggesting that some Val residues are in an in-register parallel structure and others are not (Figure 4A). This result is consistent with the one-dimensional NMR spectrum of this material that indicates approximately two-thirds of Val residues are in β-sheet structure and the remainder are not (Figure 3).

In another experiment, we labeled the methyl groups of the two Ala residues of *Ca*Ure2p$^{1-90}$ and formed amyloid in vitro. For a parallel in-register β-sheet, a nearest neighbor distance of ~5 Å is expected. Because adjacent side chains in a β-strand point in opposite directions, if the parallel β-sheet is out of register by even a single residue, the nearest neighbor distance for this side chain label will be >8 Å. The rapid signal decay seen in a PITHIRDS-CT experiment with Ala-3-^{13}C-labeled *Ca*Ure2p$^{1-90}$ (Figure 4B) is again indicative of an in-register parallel structure.

A 2D ^{13}C−^{13}C solid-state NMR experiment using uniformly ^{13}C-labeled rehydrated *Ca*Ure2p$^{1-90}$ amyloid showed broad peaks that could be assigned to only amino acid type, not to individual residues (Figure 5). This result indicates heterogeneity of structure, consistent with the heterogeneity of the prion variant observed upon transfection of yeast cells (Figure 2).

DISCUSSION

Our previous work showed that *Ca*Ure2p can form a prion in *S. cerevisiae* but that *Cg*Ure2p cannot.[40] Here we find that *Ca*Ure2p$^{1-90}$ readily forms amyloid but that *Cg*Ure2p$^{1-100}$ forms only a small amount of amyloid over a period of 2 years, providing a possible explanation for the inability of *Cg*Ure2p to be a prion. Of course, it is possible that there exists some other buffer condition under which *Cg*Ure2p would readily form amyloid. Whether amyloid forming ability (or lack of it) will be a general explanation of whether a protein can be a prion will require examination of a wide range of species.

The *Ca*Ure2p$^{1-90}$ amyloid formed is infectious for *S. cerevisiae* expressing *Ca*Ure2p in place of the *Sc*Ure2p, but we were not successful in inducing *Cg*Ure2p to form [URE3] by introducing the small amount of available *Cg*Ure2p$^{1-100}$ amyloid. Of course, it remains possible that with larger amounts of *C. glabrata* amyloids, or different conditions of amyloid formation, infection might be observed. The infection produces a variety of [URE3alb] variants with varying degrees of strong or weak phenotype and stable or unstable inheritance. This array of prion variants presumably reflects an array of amyloid structures, and the wide peaks we observe in 2D solid-state NMR experiments (Figure 5) are likely a reflection of such structural heterogeneity.

Our structural studies indicate that the amyloid fibers formed in vitro by *Ca*Ure2p$^{1-90}$ have an architecture like that of the

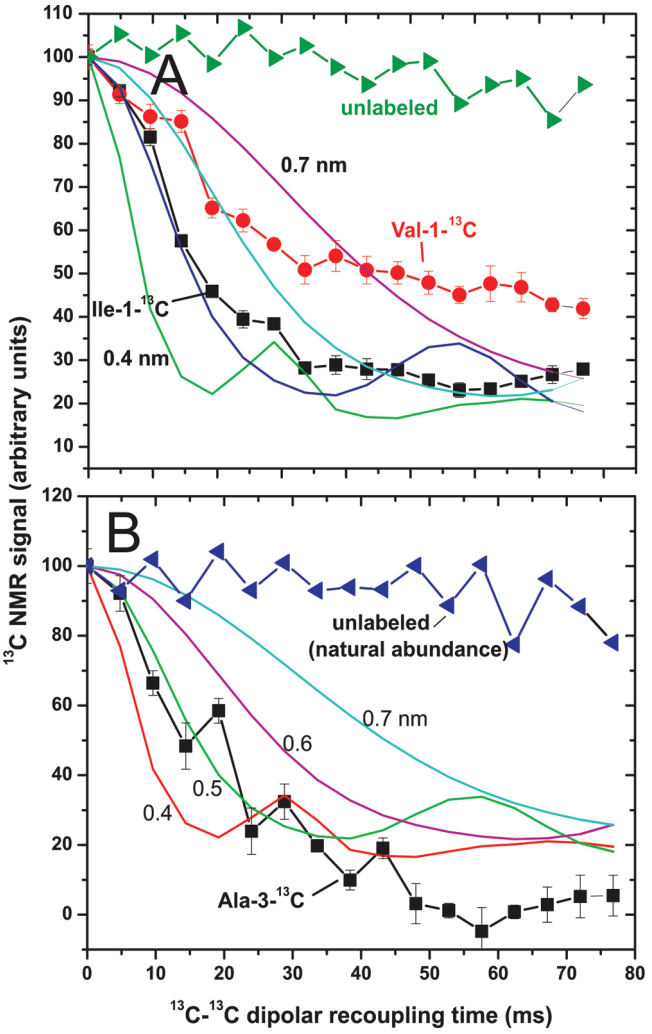

Figure 4. Dipolar recoupling experiments with selectively labeled or natural abundance *C. albicans* Ure2p$^{1-90}$ amyloid using the PITHIRDS-CT method.

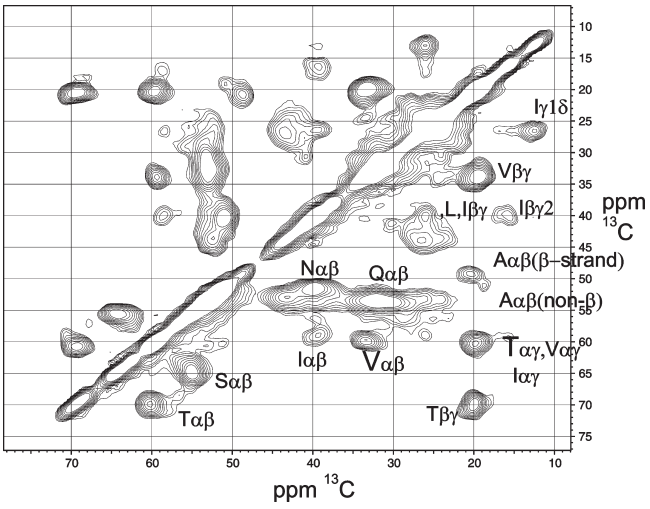

Figure 5. Aliphatic region of a $^{13}C-^{13}C$ 2D solid-state NMR spectrum of wet amyloid formed from [U-^{13}C]*Ca*Ure2p$^{1-90}$. Assignments shown do not exclude the presence in the same broad peak of signals from other residue types.

other amyloid-based yeast prions, namely, an in-register parallel β-sheet. The 6 nm diameter of the filaments of *Ca*Ure2p$^{1-90}$ indicates that the sheet is multiply folded along its long axis, because a fully extended monomer would be approximately 30 nm in length. More detailed structural studies will be needed to ascertain the location of the folds and other details of the structure, but this will require development of a method for preparing structurally homogeneous filaments.

While mammalian prions are uniformly fatal, those of yeast and fungi are not, so that whether prions are diseases or of some adaptive value must be judged by other evidence. The conservation of prion formation among closely related species would not prove that it has a function for the host (any more than the conservation of occasional broken wings among birds suggests a benefit). However, the failure of conservation among close relatives would argue against a functional role for prion formation. Residues 10−39 of the *S. cerevisiae* Ure2p prion domain are conserved among a range of yeasts,[10,11,59] and this led Harrison et al. to propose that this region is conserved to allow prion formation.[59] Ross et al. demonstrated that sequence is of little importance for the formation of prions by Ure2p or Sup35p,[35,36] so the conserved part of the Ure2p prion domain is not likely conserved for prion formation: a need for prion formation would not result in conservation of the sequence. Moreover, *C. glabrata* is closely related to *S. cerevisiae*, and *Cg*Ure2p has the conserved prion domain sequence (Figure S1 of the Supporting Information) but does not form prions. In contrast, *C. albicans* is more distantly related to *S. cerevisiae*, and its Ure2p lacks the conserved sequence (Figure S1 of the Supporting Information), but we find that it readily forms prions. This suggests that the sequence is conserved for some other reason, perhaps for the stabilization of the full-length protein by the prion domain as demonstrated for *S. cerevisiae*.[60]

While definitive data are scarce, the pattern seems to be that prion forming ability of a given protein is scattered, rather than concentrated among close relatives. For example, the full-length *S. castellii* Ure2p cannot form a prion in *S. cerevisiae*,[13] but the Ure2p's of several other *Saccharomyces* species can form [URE3]. One-fourth of wild *S. cerevisiae* strains tested had a large deletion in their Sup35 prion domains, making them unable to form the [PSI+] prion.[61] Several N-terminal domains of Sup35 of other species fused to *S. cerevisiae* Sup35C have been found to be able to act as prion domains.[16−18] However, it is known that for Ure2p, Sup35p, and HET-s, the prion domain is substantially stabilized by the remainder of the molecule,[8,19,20] so that the context of the full-length molecule is important.

The absence of the [URE3] and [PSI+] prions in wild-type strains, the inability of some species closely related to *S. cerevisiae* to form these prions, the fact that the "prion domains" have clear-cut non-prion functions, and the rapid evolution of the prion domains producing species barriers all indicate that these are yeast diseases (reviewed in ref 39). The cells themselves signal their displeasure at infection with [URE3] and [PSI+] by undergoing the stress response, inducing at least Hsp70s and Hsp104.[62,63] Moreover, the existence of lethal and very pathological variants of [PSI+] and [URE3] further argues against an adaptive role for these prions.[64] The study of these yeast prion diseases is making important contributions to our understanding of mammalian prion diseases and amyloid diseases in general.

■ ASSOCIATED CONTENT

Supporting Information. An alignment of the prion domains of Ure2p from *S. cerevisiae*, *C. albicans*, and *C. glabrata* (Figure S1). This material is available free of charge via the Internet at http://pubs.acs.org.

■ AUTHOR INFORMATION

Corresponding Author

*Bldg. 8, Room 225, NIH, 8 Center Dr., MSC0830, Bethesda, MD 20892-0830. Phone: (301) 496-3452. Fax: (301) 402-0240. E-mail: wickner@helix.nih.gov.

Funding Sources

This work was supported by the Intramural Program of the National Institute of Diabetes and Digestive and Kidney Diseases of the National Institutes of Health.

■ ACKNOWLEDGMENT

We thank Rob Tycko for help with solid-state NMR.

■ ABBREVIATIONS

Ure2^{albicans}, protein encoded by the *URE2* gene of *C. albicans*; [URE3alb], prion (infectious protein) of Ure2^{albicans}; NMR, nuclear magnetic resonance.

■ REFERENCES

(1) Wickner, R. B. (1994) [URE3] as an altered *URE2* protein: Evidence for a prion analog in *S. cerevisiae*. *Science 264*, 566–569.

(2) Derkatch, I. L., Bradley, M. E., Zhou, P., Chernoff, Y. O., and Liebman, S. W. (1997) Genetic and environmental factors affecting the *de novo* appearance of the [*PSI*+] prion in *Saccharomyces cerevisiae*. *Genetics 147*, 507–519.

(3) Derkatch, I. L., Bradley, M. E., Hong, J. Y., and Liebman, S. W. (2001) Prions affect the appearance of other prions: The story of *[PIN]*. *Cell 106*, 171–182.

(4) Du, Z., Park, K.-W., Yu, H., Fan, Q., and Li, L. (2008) Newly identified prion linked to the chromatin-remodeling factor Swi1 in *Saccharomyces cerevisiae*. *Nat. Genet. 40*, 460–465.

(5) Patel, B. K., Gavin-Smyth, J., and Liebman, S. W. (2009) The yeast global transcriptional co-repressor protein Cyc8 can propagate as a prion. *Nat. Cell Biol. 11*, 344–349.

(6) Alberti, S., Halfmann, R., King, O., Kapila, A., and Lindquist, S. (2009) A systematic survey identifies prions and illuminates sequence features of prionogenic proteins. *Cell 137*, 146–158.

(7) Masison, D. C., Maddelein, M.-L., and Wickner, R. B. (1997) The prion model for [URE3] of yeast: Spontaneous generation and requirements for propagation. *Proc. Natl. Acad. Sci. U.S.A. 94*, 12503–12508.

(8) Masison, D. C., and Wickner, R. B. (1995) Prion-inducing domain of yeast Ure2p and protease resistance of Ure2p in prion-containing cells. *Science 270*, 93–95.

(9) TerAvanesyan, A., Dagkesamanskaya, A. R., Kushnirov, V. V., and Smirnov, V. N. (1994) The *SUP35* omnipotent suppressor gene is involved in the maintenance of the non-Mendelian determinant [psi+] in the yeast *Saccharomyces cerevisiae*. *Genetics 137*, 671–676.

(10) Edskes, H. K., and Wickner, R. B. (2002) Conservation of a portion of the *S. cerevisiae* Ure2p prion domain that interacts with the full-length protein. *Proc. Natl. Acad. Sci. U.S.A. 99* (Suppl. 4), 16384–16391.

(11) Baudin-Baillieu, A., Fernandez-Bellot, E., Reine, F., Coissac, E., and Cullin, C. (2003) Conservation of the prion properties of Ure2p through evolution. *Mol. Biol. Cell 14*, 3449–3458.

(12) Talarek, N., Maillet, L., Cullin, C., and Aigle, M. (2005) The [URE3] prion is not conserved among *Saccharomyces* species. *Genetics 171*, 23–54.

(13) Edskes, H. K., McCann, L. M., Hebert, A. M., and Wickner, R. B. (2009) Prion variants and species barriers among *Saccharomyces* Ure2 proteins. *Genetics 181*, 1159–1167.

(14) Safadi, R. A., Talarek, N., Jacques, N., and Aigle, M. (2011) Yeast prions: could they be exaptations? The *URE2*/[URE3] system in *Kluyveromyces lactis*. *FEMS Yeast Res. 11*, 151–153.

(15) Hosoda, N., Kobayashii, T., Uchida, N., Funakoshi, Y., Kikuchi, Y., Hoshino, S., and Katada, T. (2003) Translation termination factor eRF3 mediates mRNA decay through the regulation of deadenylation *J. Biol. Chem. 278*, 38287–38291.

(16) Chernoff, Y. O., Galkin, A. P., Lewitin, E., Chernova, T. A., Newnam, G. P., and Belenkiy, S. M. (2000) Evolutionary conservation of prion-forming abilities of the yeast Sup35 protein. *Mol. Microbiol. 35*, 865–876.

(17) Kushnirov, V. V., Kochneva-Pervukhova, N. V., Cechenova, M. B., Frolova, N. S., and Ter-Avanesyan, M. D. (2000) Prion properties of the Sup35 protein of yeast *Pichia methanolica*. *EMBO J. 19*, 324–331.

(18) Santoso, A., Chien, P., Osherovich, L. Z., and Weissman, J. S. (2000) Molecular basis of a yeast prion species barrier. *Cell 100*, 277–288.

(19) Kochneva-Pervukhova, N. V., Poznyakovski, A. I., Smirnov, V. N., and Ter-Avanesyan, M. D. (1998) C-terminal truncation of the Sup35 protein increases the frequency of de novo generation of a prion-based [*PSI*$^+$] determinant in *Saccharmyces cerevisiae*. *Curr. Genet. 34*, 146–151.

(20) Balguerie, A., Dos Reis, S., Ritter, C., Chaignepain, S., Coulary-Salin, B., Forge, V., Bathany, K., Lascu, I., Schmitter, J.-M., Riek, R., and Saupe, S. (2003) Domain organization and structure-function relationship of the HET-s prion protein of *Podospora anserina*. *EMBO J. 22*, 2071–2081.

(21) Chernoff, Y. O., Lindquist, S. L., Ono, B.-I., Inge-Vechtomov, S. G., and Liebman, S. W. (1995) Role of the chaperone protein Hsp104 in propagation of the yeast prion-like factor [psi$^+$]. *Science 268*, 880–884.

(22) Moriyama, H., Edskes, H. K., and Wickner, R. B. (2000) [URE3] prion propagation in *Saccharomyces cerevisiae*: Requirement for chaperone Hsp104 and curing by overexpressed chaperone Ydj1p. *Mol. Cell. Biol. 20*, 8916–8922.

(23) Cox, B. S., Ness, F., and Tuite, M. F. (2003) Analysis of the generation and segregation of propagons: Entities that propagate the [PSI+] prion in yeast. *Genetics 165*, 23–33.

(24) Zenthon, J. F., Ness, F., Cox, B., and Tuite, M. F. (2006) The [PSI+] prion of *Saccharomyces cerevisiae* can be propagated by an Hsp104 orthologue from *Candida albicans*. *Eukaryotic Cell 5*, 217–225.

(25) King, C. Y., and Diaz-Avalos, R. (2004) Protein-only transmission of three yeast prion strains. *Nature 428*, 319–323.

(26) Tanaka, M., Chien, P., Naber, N., Cooke, R., and Weissman, J. S. (2004) Conformational variations in an infectious protein determine prion strain differences. *Nature 428*, 323–328.

(27) Brachmann, A., Baxa, U., and Wickner, R. B. (2005) Prion generation *in vitro*: Amyloid of Ure2p is infectious. *EMBO J. 24*, 3082–3092.

(28) Patel, B. K., and Liebman, S. W. (2007) "Prion proof" for [PIN+]: Infection with in vitro-made amyloid aggregates of Rnq1p-(132−405) induces [PIN+]. *J. Mol. Biol. 365*, 773–782.

(29) Shewmaker, F., Wickner, R. B., and Tycko, R. (2006) Amyloid of the prion domain of Sup35p has an in-register parallel β-sheet structure. *Proc. Natl. Acad. Sci. U.S.A. 103*, 19754–19759.

(30) Baxa, U., Wickner, R. B., Steven, A. C., Anderson, D., Marekov, L., Yau, W.-M., and Tycko, R. (2007) Characterization of β-sheet structure in Ure2p1−89 yeast prion fibrils by solid state nuclear magnetic resonance. *Biochemistry 46*, 13149–13162.

(31) Wickner, R. B., Dyda, F., and Tycko, R. (2008) Amyloid of Rnq1p, the basis of the [*PIN*$^+$] prion, has a parallel in-register β-sheet structure. *Proc. Natl. Acad. Sci. U.S.A. 105*, 2403–2408.

(32) Baxa, U., Taylor, K. L., Wall, J. S., Simon, M. N., Cheng, N., Wickner, R. B., and Steven, A. (2003) Architecture of Ure2p prion filaments: The N-terminal domain forms a central core fiber. *J. Biol. Chem. 278*, 43717–43727.

(33) Diaz-Avalos, R., King, C. Y., Wall, J. S., Simon, M., and Caspar, D. L. D. (2005) Strain-specific morphologies of yeast prion amyloids. *Proc. Natl. Acad. Sci. U.S.A. 102*, 10165–10170.

(34) Chen, B., Thurber, K. R., Shewmaker, F., Wickner, R. B., and Tycko, R. (2009) Measurement of amyloid fibril mass-per-length by tilted-beam transmission electron microscopy. *Proc. Natl. Acad. Sci. U.S. A. 106*, 14339–14344.

(35) Ross, E. D., Baxa, U., and Wickner, R. B. (2004) Scrambled prion domains form prions and amyloid. *Mol. Cell. Biol. 24*, 7206–7213.

(36) Ross, E. D., Edskes, H. K., Terry, M. J., and Wickner, R. B. (2005) Primary sequence independence for prion formation. *Proc. Natl. Acad. Sci. U.S.A. 102*, 12825–12830.

(37) Ross, E. D., Minton, A. P., and Wickner, R. B. (2005) Prion domains: Sequences, structures and interactions. *Nat. Cell Biol. 7*, 1039–1044.

(38) Wickner, R. B., Shewmaker, F., Kryndushkin, D., and Edskes, H. K. (2008) Protein inheritance (prions) based on parallel in-register β-sheet amyloid structures. *BioEssays 30*, 955–964.

(39) Wickner, R. B., Shewmaker, F., Edskes, H., Kryndushkin, D., Nemecek, J., McGlinchey, R., Bateman, D., and Winchester, C.-L. (2010) Prion amyloid structure explains templating: How proteins can be genes. *FEMS Yeast Res. 10*, 980–991.

(40) Edskes, H. K., Engel, A., McCann, L. M., Brachmann, A., Tsai, H.-F., and Wickner, R. B. (2011) Prion-forming abilityof Ure2 of yeasts is not evolutionarily conserved. *Genetics188*, 81–90.

(41) Brachmann, A., Toombs, J. A., and Ross, E. D. (2006) Reporter assay systems for [URE3] detection and analysis. *Methods 39*, 35–42.

(42) Christianson, T. W., Sikorski, R. S., Dante, M., Shero, J. H., and Hieter, P. (1992) Multifunctional yeast high-copy-number shuttle vectors. *Gene 110*, 119–122.

(43) Cai, M. L., Huang, Y., Sakaguchi, K., Clore, G. M., Gronenborn, A. M., and Craigie, R. (1998) An efficient and cost-effective isotope labeling protocol for proteins expressed in *Escherichia coli*. *J. Biomol. NMR 11*, 97–102.

(44) Pines, A., Gibby, M. G., and Waugh, J. S. (1973) Proton-Enhanced NMR of Dilute Spins in Solids. *J. Chem. Phys. 59*, 569–590.

(45) Bennett, A. E., Rienstra, C. M., Auger, M., Lakshmi, K. V., and Griffin, R. G. (1995) Heteronuclear Decoupling in Rotating Solids. *J. Chem. Phys. 103*, 6951–6958.

(46) Tycko, R. (2007) Symmetry-based constant-time homonuclear dipolar recoupling in solid-state NMR. *J. Chem. Phys. 126*, 064506.

(47) Petkova, A. T., and Tycko, R. (2002) Sensitivity enhancement in structural measurements by solid state NMR through pulsed spin locking. *J. Magn. Reson. 155*, 293–299.

(48) Delaglio, F., Grzesiek, S., Vuister, G. W., Zhu, G., Pfeifer, J., and Bax, A. (1995) NMRPipe: A multidimensional spectral processing system based on Unix pipes. *J. Biomol. NMR 6*, 277–293.

(49) Magasanik, B., and Kaiser, C. A. (2002) Nitrogen regulation in *Saccharomyces cerevisiae*. *Gene 290*, 1–18.

(50) Cooper, T. G. (2002) Transmitting the signal of excess nitrogen in *Saccharomyces cerevisiae* from the Tor proteins to th GATA factors: Connecting the dots. *FEMS Microbiol. Rev. 26*, 223–238.

(51) Rai, R., Genbauffe, F., Lea, H. Z., and Cooper, T. G. (1987) Transcriptional regulation of the *DAL5* gene in *Saccharomyces cerevisiae*. *J. Bacteriol. 169*, 3521–3524.

(52) Schlumpberger, M., Prusiner, S. B., and Herskowitz, I. (2001) Induction of distinct [URE3] yeast prion strains. *Mol. Cell. Biol. 21*, 7035–7046.

(53) Jung, G., Jones, G., and Masison, D. C. (2002) Amino acid residue 184 of yeast Hsp104 chaperone is critical for prion-curing by guanidine, prion propagation, and thermotolerance. *Proc. Natl. Acad. Sci. U.S.A. 99*, 9936–9941.

(54) Shewmaker, F., Kryndushkin, D., Chen, B., Tycko, R., and Wickner, R. B. (2009) Two prion variants of Sup35p have in-register β-sheet structures, independent of hydration. *Biochemistry 48*, 5074–5082.

(55) Wishart, D. S., Bigam, C. G., Holm, A., Hodges, R. S., and Sykes, B. D. (1995) H-1, C-13 and N-15 Random Coil NMR Chemical-Shifts of the Common Amino-Acids. 1. Investigations of Nearest-Neighbor Effects. *J. Biomol. NMR 5*, 67–81.

(56) Benzinger, T. L., Gregory, D. M., Burkoth, T. S., Miller-Auer, H., Lynn, D. G., Botto, R. E., and Meredith, S. C. (1998) Propagating structure of Alzheimer's β-amyloid(10−35) is parallel β-sheet with residues in exact register. *Proc. Natl. Acad. Sci. U.S.A. 95*, 13407–13412.

(57) Antzutkin, O. N., Balbach, J. J., Leapman, R. D., Rizzo, N. W., Reed, J., and Tycko, R. (2000) Multiple quantum solid-state NMR indicates a parallel, not antiparallel, organization of β-sheets in Alzheimer's β-amyloid fibrils. *Proc. Natl. Acad. Sci. U.S.A. 97*, 13045–13050.

(58) Tycko, R. (2006) Molecular structure of amyloid fibrils: Insights from solid-state NMR. *Q. Rev. Biophys. 1*, 1–55.

(59) Harrison, L. B., Yu, Z., Stajich, J. E., Dietrich, F. S., and Harrison, P. M. (2007) Evolution of budding yeast prion-determinant sequences across diverse fungi. *J. Mol. Biol. 368*, 273–282.

(60) Shewmaker, F., Mull, L., Nakayashiki, T., Masison, D. C., and Wickner, R. B. (2007) Ure2p function is enhanced by its prion domain in *Saccharomyces cerevisiae*. *Genetics 176*, 1557–1565.

(61) Resende, C. G., Outeiro, T. F., Sands, L., Lindquist, S., and Tuite, M. F. (2003) Prion protein gene polymorphisms in *Saccharomyces cerevisiae*. *Mol. Microbiol. 49*, 1005–1017.

(62) Jung, G., Jones, G., Wegrzyn, R. D., and Masison, D. C. (2000) A role for cytosolic Hsp70 in yeast [PSI+] prion propagation and [PSI+] as a cellular stress. *Genetics 156*, 559–570.

(63) Schwimmer, C., and Masison, D. C. (2002) Antagonistic interactions between yeast [PSI+] and [URE3] prions and curing of [URE3] by Hsp70 protein chaperone Ssa1p but not by Ssa2p. *Mol. Cell. Biol. 22*, 3590–3598.

(64) McGlinchey, R., Kryndushkin, D., and Wickner, R. B. (2011) Suicidal [PSI+] is a lethal yeast prion. *Proc. Natl. Acad. Sci. U.S.A. 108*, 5337–5341.